the overwhelming evidence that the depleted low velocity layer mantle source of normal ridge basalts is, to a first approximation, uniform in space and time and practically worldwide in extent (*16, 18, 20*), whereas mantles feeding oceanic islands appear to be different from one another in both rare earth and isotopic composition (*28*) and seem to have been derived from greater depths and to cover only limited areas of the oceans (*1, 29*).

SHINE-SOON SUN
*Lamont-Doherty Geological*
*Observatory of Columbia University,*
*New York 10964,* and
*Department of Earth and Space Sciences,*
*State University of New York,*
*Stony Brook 11794*
MITSUNOBU TATSUMOTO
*U.S. Geological Survey,*
*Denver, Colorado 80225*
JEAN-GUY SCHILLING
*Graduate School of Oceanography,*
*University of Rhode Island,*
*Kingston 02881*

### References and Notes

1. J.-G. Schilling, *Nature (Lond.)* **242**, 565 (1973).
2. J. T. Wilson, *ibid.* **197**, 536 (1963).
3. W. J. Morgan, *ibid.* **230**, 42 (1971).
4. S. R. Hart, J.-G. Schilling, J. L. Powell, *ibid.* **246**, 104 (1973).
5. M. J. O'Hara, *ibid.* **243**, 507 (1973).
6. J.-G. Schilling, *ibid.* **246**, 141 (1973).
7. R. K. O'Nions and R. J. Pankhurst, *Earth Planet. Sci. Lett.* **21**, 13 (1973).
8. G. E. Sigvaldason, S. Steinthorsson, N. Oskarsson, P. Imslad, *Nature (Lond.)* **251**, 579 (1974).
9. S. R. Hart and J.-G. Schilling, *Carnegie Inst. Wash. Yearb.* **72**, 259 (1973).
10. The analyses were carried out at the Denver laboratory of the U.S. Geological Survey and at the State University of New York at Stony Brook. In both cases a solid source, double focusing, 12-inch-radius mass-spectrometer of the National Bureau of Standards type, equipped with a magnetic stabilizer and computerized data acquisition system, was used. Lead samples were analyzed by the phosphate–silica gel method. The NBS 982 standard Pb was routinely measured to monitor the mass-fractionation correction. The data reported here are believed to be accurate within ± 0.1 percent for $^{206}Pb/^{204}Pb$. Concentrations of U, Th, and Pb were determined by isotopic dilution by M.T., using 1-g samples in a clean laboratory. The Pb blanks during these analyses ranged from 1.5 to 3 ng.
11. M. Tatsumoto, *J. Geophys. Res.* **71**, 1721 (1966); ——, R. J. Knight, M. H. Delevaux, *U.S. Geol. Surv. Prof. Pap. 800-D* (1972), p. 111; S. S. Sun, thesis, Columbia University (1973).
12. J.-G. Schilling and O. D. Hermes, in preparation.
13. S. S. Sun and B. M. Jahn, *Nature (Lond.)* **255**, 527 (1975).
14. H. Welke, S. Moorbath, G. L. Cumming, H. Sigurdsson, *Earth Planet. Sci. Lett.* **4**, 221 (1968).
15. For example, see T. J. Ulrych, *Science* **158**, 252 (1967); R. D. Russell, W. F. Slawson, T. J. Ulrych, P. H. Reynolds, *Earth Planet. Sci. Lett.* **3**, 284 (1967).
16. J.-G. Schilling, *J. Geophys. Res.* **80**, 1459 (1975).
17. P. W. Gast, *Geochim. Cosmochim. Acta* **32**, 1057 (1968).
18. J.-G. Schilling, *Philos. Trans. R. Soc. Lond. Ser. A Math. Phys. Sci.* **268**, 663 (1971).
19. J. R. Lancelot and C. J. Allegre, *Earth Planet. Sci. Lett.* **22**, 233 (1974). Their equation of mixing is

$$R_M = \frac{1}{C_M}\frac{C_AC_B(R_A - R_B)}{C_A - C_B} + R_B + (R_A - R_B)\frac{C_A}{C_A - C_B}$$

where $R_A$, $R_B$, and $R_M$ are any Pb isotopic ratios in mantle sources A and B and the mixture, respectively, and $C_A$ and $C_B$ are the total concentrations of lead in A and B, respectively. To calculate $R_A$ from the intercept, we used $R_B = 18.25$, the average value south of 61°N (a good estimate). On a relative basis, we estimated $C_A/(C_A - C_B)$ by using the average Pb concentration of the basalt over the Median Neovolcanic Zone of Iceland [0.702 part per million (ppm)] and south of 61°N (0.202 ppm); we assumed the same degree of partial melting, so the effect would be canceled out as it appears in both on numerator and denominator.
20. M. Tatsumoto, *Science* **153**, 1094 (1966).
21. J.-G. Schilling, in preparation. The equation for binary mixing is approximately

$$Z = \frac{(R_B - R_A)}{R_M(n - 1) - (nR_A - R_B)}$$

where $Z$ is the mass ratio of component mantles A/A + B; $R_A$, $R_B$, and $R_M$ were defined in (*19*); and $n = C_A/C_B$. Then $Z$ can be solved for various $R_M$ values for radiogenic isotope ratios or LIL element ratios observed along the transitional part of the ridge. This dependence for isotopic ratios was independently noted by J. Cann, East Anglia University, and communicated to J.-G.S.
22. G. E. Sigvaldason, *J. Petrol.* **15**, 497 (1974).
23. R. K. O'Nions and R. J. Pankhurst, *ibid.*, p. 603.
24. M. F. J. Flower, H. U. Schmincke, R. N. Thompson, *Nature (Lond.)* **254**, 404 (1975).
25. R. K. O'Nions and R. J. Pankhurst, *Earth Planet. Sci. Lett.* **21**, 13 (1973).
26. J.-G. Schilling, unpublished rare earth data for eastern Iceland; see also —— and A. Noe-Nygaard, *Earth Planet. Sci. Lett.* **24**, 1 (1974).
27. P. R. Vogt, *Earth Planet. Sci. Lett.* **13**, 153 (1971); —— and G. L. Johnson, *ibid.* **18**, 49 (1973); P. R. Vogt, in *Geodynamics of Iceland and the North Atlantic Area*, L. Kristjansson, Ed. (Reidel, Boston, 1975), p. 105.
28. For example, see (*11*); P. W. Gast, *Phys. Earth Planet. Interiors* **3**, 296 (1970); Z. E. Peterman and C. E. Hedge, *Geol. Soc. Am. Bull.* **82**, 493 (1971); C. E. Hedge, N. D. Watkins, R. A. Hildreth, W. P. Doering, *Earth Planet. Sci. Lett.* **21**, 29 (1973).
29. J.-G. Schilling, D. G. Johnson, T. H. Johnston, *Trans. Am. Geophys. Union* **55**, 294 (1974); J.-G. Schilling, *Earth Planet. Sci. Lett.* **25**, 103 (1975).
30. Supported in part by NSF grant DES 72-01705.

24 June 1975

---

# Flooding Frequency of Hypersaline Coastal Environments Determined by Orbital Imagery: Geologic Implications

Abstract. *Available satellite imagery in the infrared and near-infrared wavelengths provides a simple, rapid, and low-cost method for monitoring the extent and duration of the flooding of coastal ecosystems. Hypersaline environments in Baja California, Mexico, are flooded as a result of complex interactions between the higher of the two spring tides each month and local winds. Such flooding necessitates a reappraisal of ideas on rhythmic lamination in algal mats, stromatolites, and evaporite sediments preserved in the geologic record.*

One of the persistent problems confronting researchers in coastal processes has been the lack of repetitive data for periods of several years with observation intervals of 1 month or less. This is particularly true for remote locations. Earlier investigators of lagoons, supratidal regions, and adjacent salt flats (*1*) have reported the need for synoptic coverage of the frequency and duration of flooding of these coastal environments. Fluctuations in the areal extent of standing water contribute to the total water budget in the area and aid one in understanding subsurface refluxing and evaporation-humidity parameters. Satellite imagery, primarily the near-infrared band of LANDSAT-1 (Land Satellite) [formerly called ERTS-I (Earth Resources Technology Satellite)], in combination with field observations, is being successfully employed in our work in Baja California, Mexico, to fill this gap in previous investigations.

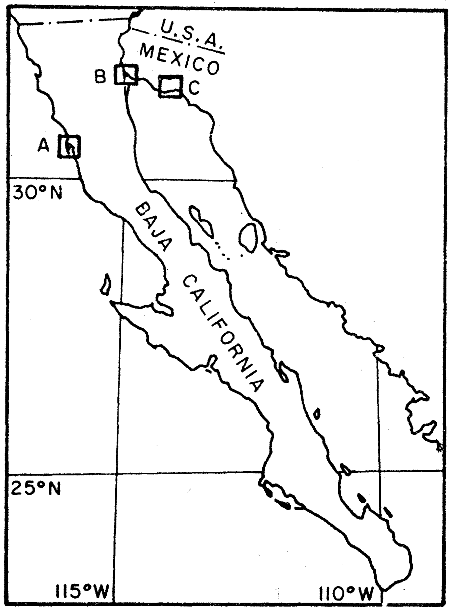

Fig. 1. Location of hypersaline deposits in Baja California, Mexico; site A, Laguna Mormona; site B, Salina Ometepec; site C, Salina Grande (Sonora).

Because infrared wavelengths penetrate water to a depth of only a few centimeters, there is a sharp contrast between water-covered surfaces and adjacent surfaces. On the basis of an analysis of the near-infrared band (0.8 to 1.1 μm) of the LANDSAT-1 multispectral scanner imagery, using a binocular microscope for zoom magnification, we were able to separate a given location (for example, the northern gypsum flat at Laguna Mormona; Fig. 1), into three classes based on a quantitative optical gray scale: (i) black, standing water; (ii) medium to dark gray, moist area; and (iii) light gray to white, dry ground. The areal percentage of each type of surface was then determined. Water bodies on the evaporite flats as small as 150 m in diameter were detectable. The technique we developed is similar to that of Reeves (*2*) who used a density control unit calibrated to a photo-

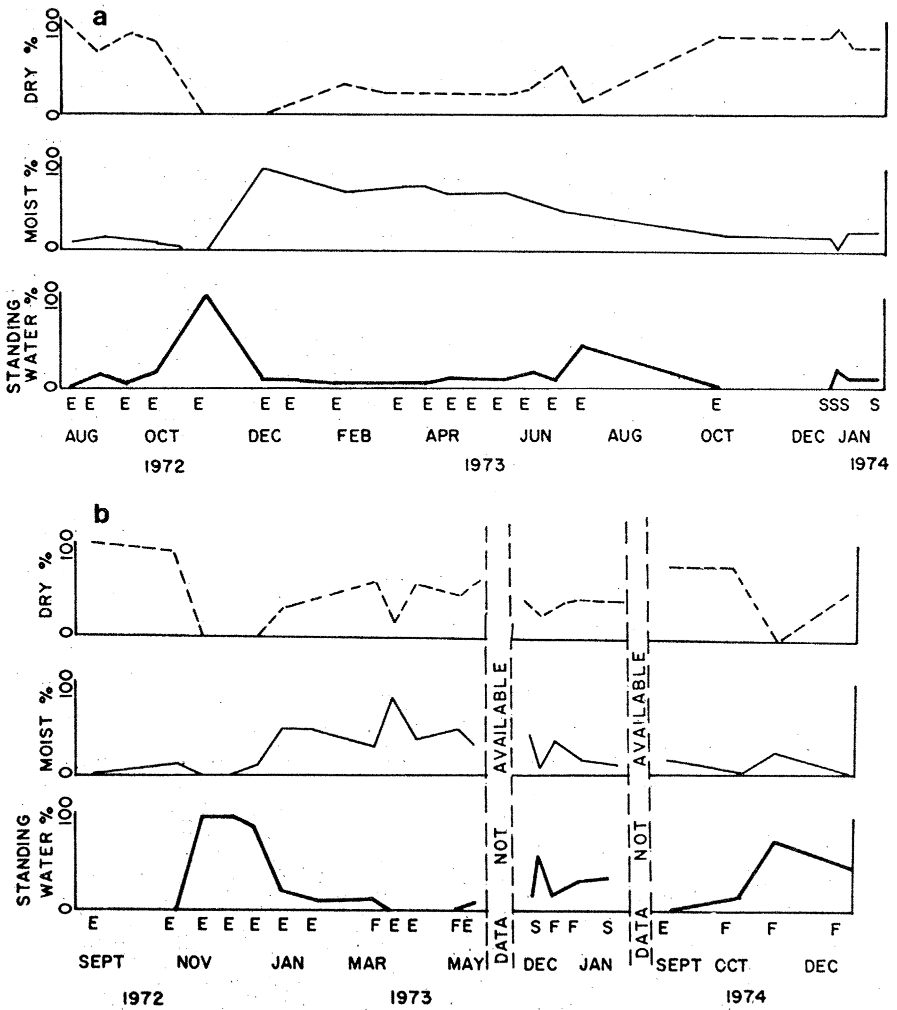

Fig. 2. Flooding frequency and duration at Salina Ometepec (a) and Laguna Mormona (b), showing flooding pulses and variable moist-dry area conditions for the period from August 1972 through December 1974 (Mormona) and through January 1974 (Ometepec). Symbols: *S*, data from Skylab; *F*, data from field observations; and *E*, data from LANDSAT.

graphic step wedge for studying lake basins on the Texas High Plains. Infrared photographs from the Skylab missions were also used in our study, and field observations were conducted during times of key overflights to provide ground truth.

Laguna Mormona, Salina Ometepec, and Salina Grande (Fig. 1) were the hypersaline environments used as test sites. The data for Salina Grande parallel the data for Salina Ometepec which are presented here. The Mormona complex is separated from the Pacific Ocean by an unbreached barrier-dune ridge with water percolating into the lagoons and nearby salt flats through and under the dunes. Salina Ometepec, on the western edge of the Colorado Delta tide flats in the Gulf of California, is primarily an area of halite-gypsum deposition (*3, 4*) as compared to the gypsum-algal mat-stromatolite associations (stromatolites are organosedimentary structures built by blue-green algae) of Laguna Mormona (*5*). Variations in the flooding of the upper Gulf of California site were initially documented by infrared and other orbital photography from the Gemini and Apollo missions (*6*). Only with the advent of the LANDSAT-1 imagery on 18-day intervals, however, was synoptic data available for long-term correlation and comparison with the Pacific coastal area.

Surface flooding of these Baja California coastal areas (Fig. 2) does not correlate in any simple manner with spring tides, persistent onshore winds, storms, seasonal rains, hurricanes, tectonic movement, or seasonal changes in sea level as suggested previously (*1, 3, 4, 7*). Complete flooding of the environments occurred during November 1972; only partial flooding occurred in July and December 1973 and October 1974 (Fig. 2). Areas for which all flooding pulses are recorded in terms of the precipitation of evaporite minerals or algal growth are thus in gradational lateral continuity with areas for which only the major flooding in November 1972 is recorded. Although there is a general inverse relationship between flooded and dry portions, on some occasions, such as March–April 1973 (Fig. 2b), moist sections persisted. These moist sections are of crucial importance because within them the sediments undergo solution and recrystallization that obscure laminar precipitations from the bodies of standing water. On the basis of field observations we believe that a complex interaction between the higher of the two spring tides each month and local winds is the dominant cause of flooding, but precise meteorological data have not been available for these remote areas.

The principal implications appear to be the following:

1) Although laminated gypsum and bedded gypsum have been thought to be a criterion for precipitation from standing bodies of evaporating water (*8*), they also form during early diagenesis within the sediment (*4, 5*). Cyclicity in such evaporites has been the subject of extended controversy (*9*) and has been used to indicate periodic climatic, solar, and tectonic fluctuations. The satellite data (Fig. 2) confirm and elaborate on the suggestion (*4*) that rhythmic bedding of halite-gypsum in the coastal setting is apparently related to erratic and nonseasonal rather than to regular and annual flooding by marine waters.

2) Investigations of laminae in algal mats and stromatolites (*10*) have focused on research into the development and diversity of Precambrian life (*11*), and have been given impetus by application to plate tectonics and geosynclinal theory (*12*). Details on the mode of origin of these laminites, like those of the cyclic evaporites, have been subject to a multiplicity of conflicting interpretations. Although present-day algal mats (30 cm thick) at Laguna Mormona exhibit rhythmic laminae, marking studies with the use of Carborundum powder indicate an extreme variation in laminae formation (*5*). These laminae are not simply related to tidal or seasonal changes but rather are due to a more intricate combination of desiccation and flooding as documented in Fig. 2.

STEPHEN P. VONDER HAAR
DONN S. GORSLINE
*Department of Geological Sciences,*
*University of Southern California,*
*Los Angeles 90007*

### References and Notes

1. F. B. Phleger and G. C. Ewing, *Geol. Soc. Am. Bull.* **73**, 145 (1962); D. J. J. Kinsman, *Am. Assoc. Petrol. Geol. Bull.* **53**, 830 (1969); G. M. Friedman, A. J. Amiel, M. Braun, D. S. Miller, *ibid.* **57**, 541 (1973).
2. C. C. Reeves, Jr., in *Third ERTS-1 Symposium* (Special publication 351, National Aeronautics and Space Administration, Washington, D.C., 1973), section B, vol. 1, p. 1041.
3. R. W. Thompson, *Geol. Soc. Am. Mem. 107* (1968), p. 21.
4. D. J. Shearman, *Inst. Min. Metall. Trans. Sect. B* **79**, B155 (1970); S. M. B. Smith, in preparation.
5. R. Horodyski and S. P. Vonder Haar, *J. Sediment. Petrol.*, in press; S. P. Vonder Haar, thesis, University of Southern California (1972).
6. S. P. Vonder Haar and R. O. Stone, *Photogram-*

*metria* **29**, 45 (1973); R. O. Stone, L. D. Carter, S. P. Vonder Haar, *Z. Geomorphol. Suppl. Neue Folge* **18**, 156 (1973).
7. M. Nichols *et al.*, "Sequential photography for coastal oceanography" (Virginia Institute of Marine Science, Williamsburg, November 1972).
8. F. J. Lucia, *Soc. Econ. Paleontol. Mineral. Spec. Publ. 16* (1974), p. 160.
9. P. Duff, A. Hallam, E. K. Walton, *Cyclic Sedimentation* (Elsevier, Amsterdam, 1967), pp. 199–214.
10. B. W. Logan, R. Rezak, R. N. Ginsburg, *J. Geol.* **72**, 68 (1964); S. M. Awramik, *Science* **174**, 825 (19→ P. Hoffman, *ibid.* **157**, 1043 (1967).
→ J. W. Schopf, *Origins Life* **5**, 119 (1974).
12. P. Hoffman, *Am. Assoc. Petrol. Geol. Bull.* **58**, 856 (1974).
13. Research was supported in part by a grant from the Geological Society of America, a research grant from the American Association of Petroleum Geologists, and contract N00014-67-A-0269-0009 of the Geography Programs, Office of Naval Research. We thank H. W. Stumpf for his assistance in obtaining the imagery in the early parts of the research program.

30 May 1975

# Hydrogen Cyanide Production During Reduction of Nitric Oxide over Platinum Catalysts

Abstract. *The catalytic reduction of nitric oxide with carbon monoxide and hydrogen was studied with a bench-scale flow reactor at 400° to 800°C over platinum to determine the yield of hydrogen cyanide. An opto-acoustic infrared absorption technique was applied to the analysis of hydrogen cyanide. In mixtures of nitric oxide, carbon monoxide, hydrogen, and water vapor, with all concentrations in the range of 0.1 to 5 percent, up to 80 parts per million (ppm) of hydrogen cyanide is formed over platinum at 600° to 800°C. In the absence of water vapor, the hydrogen cyanide concentration rises to 700 ppm. With 6 to 60 ppm of sulfur dioxide in the gas mixture, hydrogen cyanide production is suppressed to less than 5 ppm. No significant differences were found between a platinum sponge and platinum supported on cordierite. The implications of our results for the catalytic treatment of automotive exhaust are examined.*

The chemistry of NO at low concentrations is of importance in atmospheric chemistry and in air pollution abatement. For these reasons, we have measured the kinetics of the reactions of NO with CO and $H_2$ over metallic (*1*) and oxidic (*2*) catalysts, employing synthetic mixtures of the pure compounds diluted with He and using bench-scale catalytic flow reactors. For similar reasons, we have developed selective and sensitive opto-acoustic (OA) infrared absorption techniques, using tunable (*3*) and fixed-frequency lasers (*4*). In the work reported here we combined these techniques to study the formation of HCN in synthetic mixtures of NO, CO, $H_2$, $H_2O$, and $SO_2$ diluted with He (when reduced over Pt catalysts at 400° to 800°C). The choice of the Pt catalyst was based on the following considerations.

Abatement of automotive exhaust emissions in the United States relies heavily on the use of catalytic converters in which CO and hydrocarbons are oxidized to $CO_2$ and $H_2O$ (*5*). Presently used catalysts contain Pt as the active ingredient. They operate predominantly under net *oxidizing* conditions. However, under some driving modes, net *reducing* conditions may prevail, for example, in deceleration or downhill coasting. Indeed, $H_2S$ derived from the reduction of $SO_2$ in the exhaust has been observed during such transients (*6*, p. 92). Future application of catalytic converters for the reduction of $NO_x$ (oxides of nitrogen) is a strong possibility, especially in the remainder of this decade (*5*). In some proposed devices for $NO_x$ reduction, a Pt catalyst is used in a reducing exhaust mixture as an oxygen scavenger upstream from the proper $NO_x$ catalyst (*6*, p. 41). We have recently observed HCN in the reaction products from the reduction of NO by CO and $H_2$ in synthetic gas mixtures over Pt catalysts. In the following we describe the identification of HCN by gas chromatography (GC), mass spectrometry (MS), highly selective infrared (IR) absorption, and chemical analysis. Also, we report the parameters affecting the yield of HCN, such as temperature, gas composition, and flow rate (*7*).

The Pt catalysts used included a gently crushed honeycomb catalyst (Pt-I) containing approximately 0.2 percent Pt (by weight) on an alumina wash coat on cordierite support (*8*). The Pt area per gram of catalyst Pt-I was 0.07 $m^2$, as determined by chemisorption of $H_2$ (*9*). The other catalyst used was a Pt "sponge" (Pt-II) with a specific surface area of 0.12 $m^2/g$, as determined by the BET (Brunauer, Emmett, and Teller) $N_2$ adsorption technique (*9*). The HCN was produced in a continuous-flow, fixed-bed quartz reactor, when mixtures of CO (3 to 5 percent), NO [1500 to 3000 parts per million (ppm)], $H_2$ (0.2 to 0.5 percent), $H_2O$ (0 to 4 percent), and $SO_2$ (0 to 60 ppm) diluted with He were passed through the catalyst, which was supported by a porous quartz disk. Automatic sampling of the effluent at 15-minute intervals was coupled with on-line injection into two gas chromatographs. In one gas chromatograph, incorporating a 4.9-m Porapack R column at 109°C, HCN, $NH_3$, $H_2O$, and $CO_2$ were measured. The HCN was identified by the calibrated retention time and peak shape; HCN in He (approximately 1000 ppm) served for calibration (*10*). This method was applied only for low concentrations of $H_2O$ in the effluent ($\leqq$ 0.5 percent) because of the reduced sensitivity for HCN in the presence of $H_2O$. The second gas chromatograph contained molecular sieve 13x and Porapack Q columns at 30°C for the separation of $N_2$, NO, CO, $H_2$, $N_2O$, and $CO_2$ in the dried effluent (*1*). For both gas chromatographs, thermal-conductivity detectors were used. Samples of the reactor effluent were analyzed and HCN was identified therein by MS, yielding peaks at a mass-to-charge ratio $m/e$ of 26 and 27 (*11*). The identifications by MS and GC were not considered sufficient, since other compounds might fortuitously yield the same retention time in the gas chromatograph or the same peaks in the mass spectrometer. Therefore, in several instances, the effluent from the reactor was bubbled through an excess KOH solution to bind $CO_2$ and HCN for 16 hours and the solution was analyzed for $CN^-$ by the Liebig method (*12*).

Table 1. Relative sensitivities for the detection of HCN and $H_2O$ (normalized to power level on each of the laser lines) at a total gas pressure of 60 torr in the OA cell.

| CO laser | | OA signal | |
|---|---|---|---|
| Line | Frequency ($cm^{-1}$) | HCN (1000 ppm) | $H_2O$ (10000 ppm) |
| $P_{27-26}(12)$ | 1442.15 | 50.0 | $<10^{-3}$ |
| $P_{26-25}(15)$ | 1456.02 | $<10^{-5}$ | 4.8 |

Definitive identification and quantitative determination of HCN were made by IR absorption with OA detection. The effluent gas flowed continuously through the OA cell, which was connected to the reactor by stainless steel tubing. The IR detection of minute concentrations of pollutant gases has recently been studied with both tunable-frequency (*3*) and fixed-frequency (*4*) IR lasers. Detection of HCN, however, is difficult, especially in the presence of high concentrations of $H_2O$ vapor, because of the relative inaccessibility of the IR active fundamental vibrational bands of HCN. The $\nu_2$ fundamental centered at ~712 $cm^{-1}$ (*13*) and the $\nu_3$ fundamental centered at ~3312 $cm^{-1}$ (*14*) are in ranges where tunable lasers with continuous wave (cw) power output sufficient for OA spectroscopy are not available. The alternative, a dense packing of fixed-frequency laser lines, is also not available in these ranges (*15*). We have therefore used the coincidence of the HCN $2\nu_2$ absorption band at ~1411 $cm^{-1}$ (*13*) with the fixed-frequency lines of a CO laser (*16*).

The weakness of the absorption due to the $2\nu_2$ band relative to that arising from